Development 137, 1067-1073 (2010) doi:10.1242/dev.041434

Planar cell polarity defects and defective Vangl2 trafficking in mutants for the COPII gene *Sec24b*

Carolien Wansleeben[1,*], Harma Feitsma[1], Mireille Montcouquiol[2], Carla Kroon[1], Edwin Cuppen[1] and Frits Meijlink[1,*]

SUMMARY

Among the cellular properties that are essential for the organization of tissues during animal development, the importance of cell polarity in the plane of epithelial sheets has become increasingly clear in the past decades. Planar cell polarity (PCP) signaling in vertebrates has indispensable roles in many aspects of their development, in particular, controlling alignment of various types of epithelial cells. Disrupted PCP has been linked to developmental defects in animals and to human pathology. Neural tube closure defects (NTD) and disorganization of the mechanosensory cells of the organ of Corti are commonly known consequences of disturbed PCP signaling in mammals. We report here a typical PCP phenotype in a mouse mutant for the *Sec24b* gene, including the severe NTD craniorachischisis, abnormal arrangement of outflow tract vessels and disturbed development of the cochlea. In addition, we observed genetic interaction between *Sec24b* and the known PCP gene, scribble. Sec24b is a component of the COPII coat protein complex that is part of the endoplasmic reticulum (ER)-derived transport vesicles. Sec24 isoforms are thought to be directly involved in cargo selection, and we present evidence that Sec24b deficiency specifically affects transport of the PCP core protein Vangl2, based on experiments in embryos and in cultured primary cells.

KEY WORDS: COPII-mediated protein trafficking, Planar cell polarity, Neural tube closure defect, Mouse genetics, Inner ear development, Cardiac defects

INTRODUCTION

Correct polarization and orientation of cells is of crucial importance for their function. In addition to apical-basal polarization, cells may be polarized in an orthogonal orientation, often but not exclusively in the plane of an epithelial sheet (Wu and Mlodzik, 2009). Loss of this planar cell polarization (PCP) has been correlated with developmental defects as well as with tumorigenesis (Humbert et al., 2003; Saburi et al., 2008; Zhan et al., 2008).

PCP signaling not only determines planar asymmetry of a cell, but also the ability of the cell to propagate this polarity to adjacent cells, thus establishing tissue polarity. It was originally discovered and studied in *Drosophila*, but in recent years the significance of PCP signaling for vertebrate development has become increasingly clear. Developmental processes involving PCP include the convergent extension movements that shape the embryo during gastrulation and neurulation, and the regular arrangement of structures as diverse as stereocilia in the organ of Corti and epidermal hairs (Wang and Nathans, 2007; Montcouquiol et al., 2003; Devenport and Fuchs, 2008). Mouse mutant embryos with a disrupted PCP pathway frequently suffer from the extreme neural tube closure defect known as craniorachischisis, which is rarely, if at all, encountered outside this context (Kibar et al., 2001; Curtin et al., 2003) (reviewed by Copp et al., 2003). PCP pathways in insects and vertebrates share a core pathway that includes members of the dishevelled and frizzled gene families, but which is distinct from the β-catenin-dependent 'canonical' Wnt pathway (Lawrence et al., 2007).

In a random mutagenesis screen for genes essential for normal mouse development, we have identified a series of mutant lines on the basis of their abnormal appearance at day 10.5 of gestation. Of two mutants displaying craniorachischisis, one was shown to carry a novel mutant allele of the known PCP gene scribble (*Scrib*), whereas the second was found to be allelic with the *Sec24b* gene, which encodes a component of the coat protein complex II (COPII) that is essential for intracellular endoplasmic reticulum (ER)-to-Golgi protein transport (Sato and Nakano, 2007). This suggests a link between protein trafficking and PCP signaling, which would indicate an unexpected level of specificity in the process of cargo selection by Sec24 isoforms. *Sec24b* loss-of-function probably causes a deficiency in the transport of one or more membrane proteins involved in planar polarity and we present evidence that van gogh-like2 (Vangl2) is among these.

MATERIALS AND METHODS

Mouse strains and identification of mutants

Mutants were generated by random chemical mutagenesis and mapped using procedures essentially similar to those used by Kasarskis (Kasarskis et al., 1998) and to be published elsewhere in more detail (C.W., Van Gurp, L., H.F., C.K., Rieter, E., Verberne, M., Guryev, V., E.C. and F.M., unpublished). Briefly, C57BL/6 mice were injected three times at 1-week intervals with 60-80 mg/kg bodyweight of ethyl-N-nitrosurea (ENU) and after recovery, crossed to FVB/N mice. The resulting male founders were crossed with their daughters and embryos were visually inspected on embryonic day (E) 10.5. A SNP panel distinguishing C57BL/6 and FVB/N polymorphisms was used for positional cloning of the affected genes. Animal experiments were conducted under the approval of the Animal Care Committee of the KNAW.

Histology and immunostaining

Embryos and inner ears were dissected in PBS and fixed for 2 hours in 2% paraformaldehyde (PFA) for immunostaining and in 4% PFA overnight for Hematoxylin and Eosin stainings and in situ hybridizations. Cochleae were dissected and the organ of Corti was revealed by removing the stria vascularis. Stereocilia were visualized by staining with Rhodamin-

[1]Hubrecht Institute, KNAW & University Medical Center Utrecht, Uppsalalaan 8, 3584 CT Utrecht, The Netherlands. [2]INSERM U862, Université Bordeaux II, 146 rue Léo-Saignat, 33077 Bordeaux Cédex, France.

*Authors for correspondence (c.wansleeben@hubrecht.eu; f.meijlink@hubrecht.eu)

Accepted 22 January 2010

Phalloidin (Cytoskeleton Inc., Denver, CO, USA) or Phalloidin-Alexa Fluor 633 (Invitrogen). DNA was stained with DAPI (Invitrogen). Immunohistochemistry to detect PECAM, including zinc fixation, was exactly as described by Van Nes (Van Nes et al., 2006). Vangl2 staining was as described by Montcouquiol (Montcouquiol et al., 2006; Montcouquiol et al., 2008). Ptk7 staining was as described by Lu (Lu et al., 2004). Myo7A (Proteus) and E-cadherin (Transduction Laboratories) antibodies were used as 1:200 and 1:1000 dilutions, respectively. In situ hybridization was as described previously (Kuijper et al., 2005).

Transfection

Mouse embryo fibroblasts (MEFs) were prepared according to standard procedures and cultured in DMEM + 10% fetal calf serum (FCS), trypsinized at 60-70% confluency and plated at a 1:4 dilution into square 25-well dishes (4 cm^2/well) containing 18 mm diameter gelatin-coated glass coverslips. After culturing for 16-24 hours, medium was replaced by serum-free medium for 1 hour. DNA construct at 0.75 μg or 1.5 μg was mixed with 1 ml serum-free medium and incubated for 10 minutes and then mixed with a 5-fold (w/w) excess of polyethylenimine (PEI, Polysciences Inc.) from a 1 mg/ml stock solution in water and left for 30 minutes at room temperature. Subsequently, the mixture was added to the 25-well dish and left for three hours at 37°C at 5% CO_2, after which it was replaced by DMEM with 10% FCS for 21 hours. Fixation on the coverslips was for 30 minutes at room temperature in 4% PFA in PBS. Fluorescence was analyzed by using a Leica TCS SPE confocal microscope and the Leica Application Suite software.

pEGFP-Vangl2 was described previously (Montcouquiol et al., 2006). The coding region of *Tspan2* was amplified by PCR from total mouse embryo cDNA and cloned into the *pEGFP-C3* vector. The CAAX-YGFP construct was a gift of J. Bussmann (Hubrecht Institute); it encodes the Ras prenylation signal KLNPPDESGPGCMSCKCVLSX fused to YGFP.

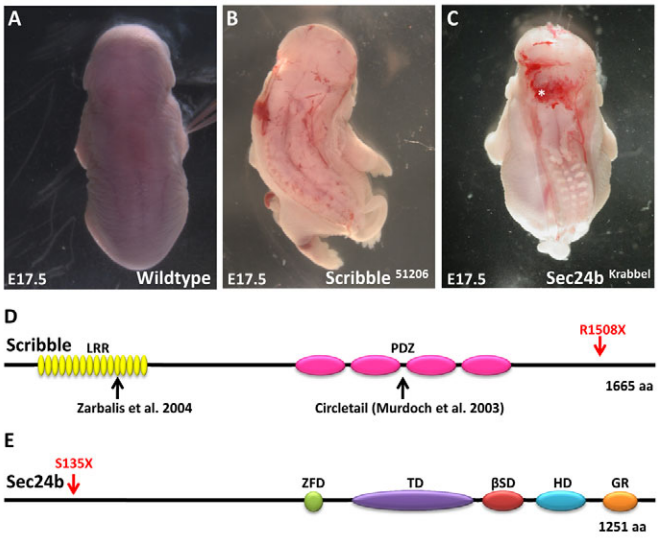

Fig. 1. Mutations in *Scrib* and *Sec24b* lead to craniorachischisis. (**A-C**) Dorsal views of E17.5 foetuses showing open neural tubes in both mutants. Note the typical rightward kink in the *Scrib* foetus also noted by Murdoch (Murdoch et al., 2001). The asterisk in C indicates local blood effusions. (**D**,**E**) Schematic representation indicating *Scrib*^{51206} and *Sec24b*^{krabbel} alleles. The structure of the encoded proteins is shown, with conserved domains depicted as coloured shapes. Red arrows indicate the location of truncation described in this paper and black arrows point to previously reported *Scribble* mutations.

RESULTS AND DISCUSSION

Identification and mapping of two craniorachischisis mutants

Two mutant lines characterized by craniorachischisis, tentatively named 51206 and krabbel, were identified in a genetic screen in mouse (Fig. 1A-C). This phenotype is often associated with disruption of PCP signaling. Genetic mapping of the 51206 allele resulted in the identification of an interval on chromosome 15 between 71 and 83.2 Mbp, containing the scribble (*Scrib*) gene, which has previously been linked to craniorachischisis and gastroschisis (Rachel et al., 2002; Murdoch et al., 2001; Murdoch et al., 2003; Zarbalis et al., 2004). Sequencing of the 38 exons of *Scrib* revealed a C to T transition of nucleotide 4865 (ENSMUST00000002603) in exon 33, resulting in a nonsense mutation of arginine 1508 that truncates the protein by 158 amino acids (Fig. 1D). We conclude that this mutation is responsible for the affected phenotype. All conserved domains of *Scrib*, including the 16 leucine-rich repeats and four PDZ domains, are left intact by the mutation and a specific function of the carboxy-terminus has not been reported (Albertson et al., 2004), leaving the possibility that this is not a null allele, in spite of the strong phenotype. Quantitative PCR (qPCR) experiments (data not shown) revealed an approximately 65% decrease of *Scrib* mRNA in mutant embryos, presumably attributable to nonsense-mediated decay (NMD) (Stalder and Mühlemann, 2008). Therefore, the function of the protein encoded by the *Scrib*^{51206} allele might be affected both qualitatively and quantitatively.

Genetic mapping of the krabbel mutation identified a 9.24 Mb segment of chromosome 3 expected to contain the mutation. By sequencing the exons of the genes in this segment, we discovered a C to A transversion at genomic position 3:129705867, which corresponds to nucleotide 304 of exon 2 of the *Sec24b* gene. The occurrence of the mutation correlated completely with the krabbel phenotype in well over 100 mutant embryos. According to the ENSEMBL database, the *Sec24b* gene (ENSMUSG00000001052) encodes two transcripts owing to alternative splicing, ENMUST00000001079 and ENMUST00000098616. The mutation changes a Ser codon to a stop codon, removing 1117 of the 1251 or 1082 of the 1216 amino acids of the two Sec24b protein variants, respectively. As the mutation is upstream from the alternatively spliced exon, the same residual 134-amino acid peptide remains, encoded by both splice variants. This allele must therefore represent a null (Fig. 1E). The expected NMD effect on *Sec24b* mRNA concentration was confirmed by qPCR, and estimated to be 72% (data not shown). While this manuscript was under review, Merte et al. (Merte et al., 2010) independently reported a different *Sec24b* mutant with a craniorachischisis phenotype. The existence of a second mutant allele definitely establishes the link between *Sec24b* and craniorachischisis.

Sec24b encodes a component of the COPII complex that has an essential role in generating secretory vesicles at the ER. These vesicles have a central function in the strictly regulated ER–Golgi secretory pathway (Salama and Schekman, 1995; Fromme and Schekman, 2008). Genetic work in yeast has uncovered a series of genes that encode the various constituents of the COPII coat (Kuehn and Schekman, 1997). Sec24, occurring as a component of Sec23-Sec24 dimers, has been linked specifically to a function in cargo selection. *Sec24b* is one of four paralogous genes, which are found in mouse, human and other vertebrate genomes. Knowledge of any distinct functional specificity of these four genes remains rather limited (see Wendeler et al., 2007). In the early embryo (at least E8.5-E10.5) all four paralogues, with the possible exception of *Sec24d*, are ubiquitously expressed (see Fig. S1 in the supplementary material).

Sec24b^{krabbel} mutants fail to undergo neural tube closure

At least 95% of *Sec24b*^{krabbel} mutant embryos displayed severe neural tube closure defects, whereas the remaining fraction had a weaker but similar phenotype. We observed gastroschisis in less than 5% of *Sec24b*^{krabbel} mutant foetuses, in contrast to the *Scrib*^{51206} mutant that displayed this failure of the ventral body wall to close in about half of the embryos (see also Murdoch et al., 2003).

Aberrant aortic arch morphology in *Sec24b*^{krabbel} mutants

Homozygous *Sec24b*^{krabbel} mutant foetuses die around day E17.5 of gestation and are externally recognized by blood-filled yolk sacs and local effusions (Fig. 1C, asterisk) indicative of disturbed blood circulation.

Several mouse mutants known to have deficient PCP signaling have been shown to have severe cardiac abnormalities (reviewed by Van den Hoff and Moorman, 2005; Henderson et al., 2006; Davis and Katsanis, 2007). Numerous aspects of cardiogenesis may be affected in PCP mutants, often including outflow tract abnormalities like double-outlet right ventricle, misplacement of the great arteries, aortic arch abnormalities and septation defects. Possible explanations for these aberrancies include defects in directed cell migration due to disrupted PCP signaling, deficient 'myocardialization' of some of the great vessels, and looping defects.

To see whether *Sec24b*^{krabbel} mutants display any of these abnormalities, we compared cardiac development of mutant and wild-type embryos. Fig. 2A compares PECAM-stained E16.5 hearts from a wild-type embryo and a *Sec24b*^{krabbel} mutant. Ventricles were abnormally small in mutants, whereas dissection of atria demonstrated approximately normal sizes in mutants (data not shown). In addition, as the appearance of the great outflow vessels gave some indication of their abnormal orientation in the mutant, we decided to investigate this further by analysis of histological sections. Transverse sections of E15.5 hearts revealed an abnormal arrangement of the vessels branching off from the aortic arch. Although in the wild-type heart (Fig. 2B,D) the subclavian artery can be seen to be located ventrally from the oesophagus and trachea, in the mutant this artery branches off of the aortic arch at an abnormal position and is at a dorsal position from the oesophagus and trachea (Fig. 2C,E), an anomaly known as retroesophageal subclavian artery (RSA). In addition, in sections at a more caudal level, we observed that the pulmonary artery was directed in an aberrant, rightward direction (see Fig. 2F,G).

RSA is among the abnormalities reported for embryos carrying mutations in PCP genes: Torban and colleagues (Torban et al., 2008) observed RSA in *Vangl2* mutants, where it is accompanied by severe cardiac septation defects. Interestingly, V*angl2*/*Vangl1* double-heterozygous embryos had RSA as the predominant effect.

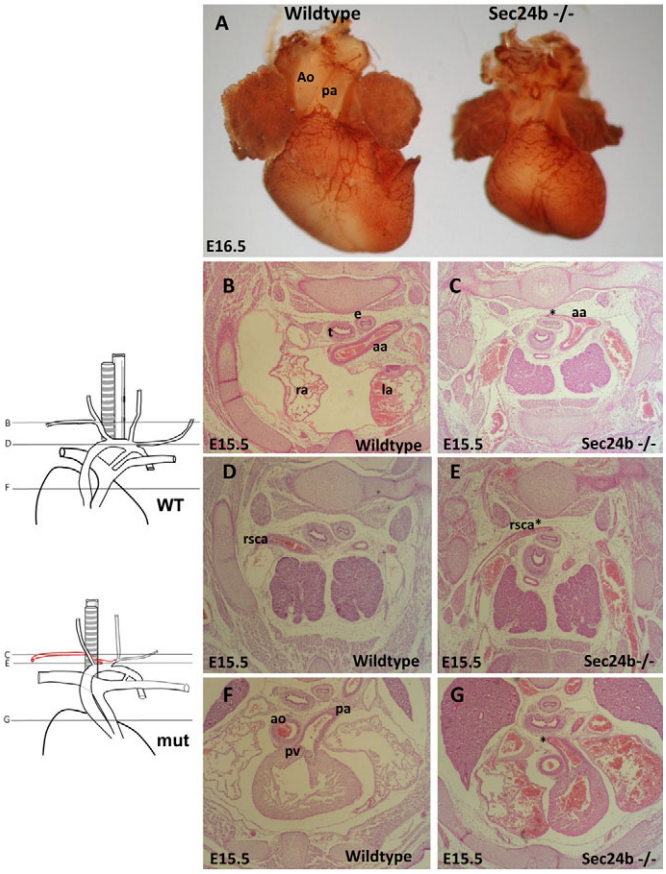

Fig. 2. Cardiac phenotype in *Sec24b*^{krabbel} mutant. (**A**) Frontal view of wild-type and *Sec24b*^{krabbel} mutant hearts at E16.5, demonstrating ventrical size differences and suggesting abnormalities of the pulmonary artery and aorta. The hearts were stained with an anti-PECAM antibody. (**B-G**) Histological sections demonstrating cardiac defect of *Sec24b* mutant embryos (C,E) compared with wild types (B,D). The diagram to the left of these panels represents our interpretation of the phenotype while indicating the level of the sections, with the mutant right subclavian artery in red. More-rostral sections show the normal position of the right subclavian artery (marked rsca in D) and the abnormal position, dorsal from the esophagus and the trachea (marked rsca* in E). In more-caudal sections, the abnormal location of the site where the subclavian branches off of the aortic arch in the mutant is indicated with an asterisk (C). The aorta and pulmonary artery are separated, demonstrating the absence of a double-outlet ventricle, but an abnormal rightward orientation of the pulmonary artery (asterisk in G) is obvious (F,G). aa, aortic arch; Ao, aorta; e, esophagus; la, left atrium; lv, left ventricle; pa, pulmonary artery; pv, pulmonary valve; ra, right atrium; rsca, right subclavian artery; rv, right ventricle; t, trachea.

Sec24b^{krabbel} mutants have smaller cochleae and an abnormal arrangement of hair cells in the organ of Corti

A classic manifestation of planar polarity in mammals occurs in the development of the inner ear. PCP mutants may have shorter cochlear tubes and, in addition, misalignment of cochlear mechanosensory receptors, i.e. the stereociliary bundles of the organ of Corti (Montcouquiol et al., 2003; Curtin et al., 2003).

Dissection at E16.5 of inner ears of *Sec24b*^{krabbel} mutant foetuses revealed that mutant cochleae were markedly smaller than those from wild-type and heterozygous embryos. Although an extensive analysis of the vestibular system is beyond the scope of the present study, we tentatively conclude that it appears relatively normal (Fig. 3A,B). To obtain an objective quantitative measure for reduction of cochlear duct length, we measured the length of the organ of Corti by means of stainings for the hair cell marker Myo7A (Fig. 3C). This confirmed that the lengths of organ of Corti in *Sec24b* and *Scrib* mutants were reduced by a statistically significant degree (Fig. 3D). Comparable observations have previously been reported for PCP mutants, including *Vangl2* (Torban et al., 2008) and double mutants involving *Dvl1-3* genes (Wang et al., 2005; Etheridge et al., 2008). This prompted us to investigate in these cochleae the stereociliary

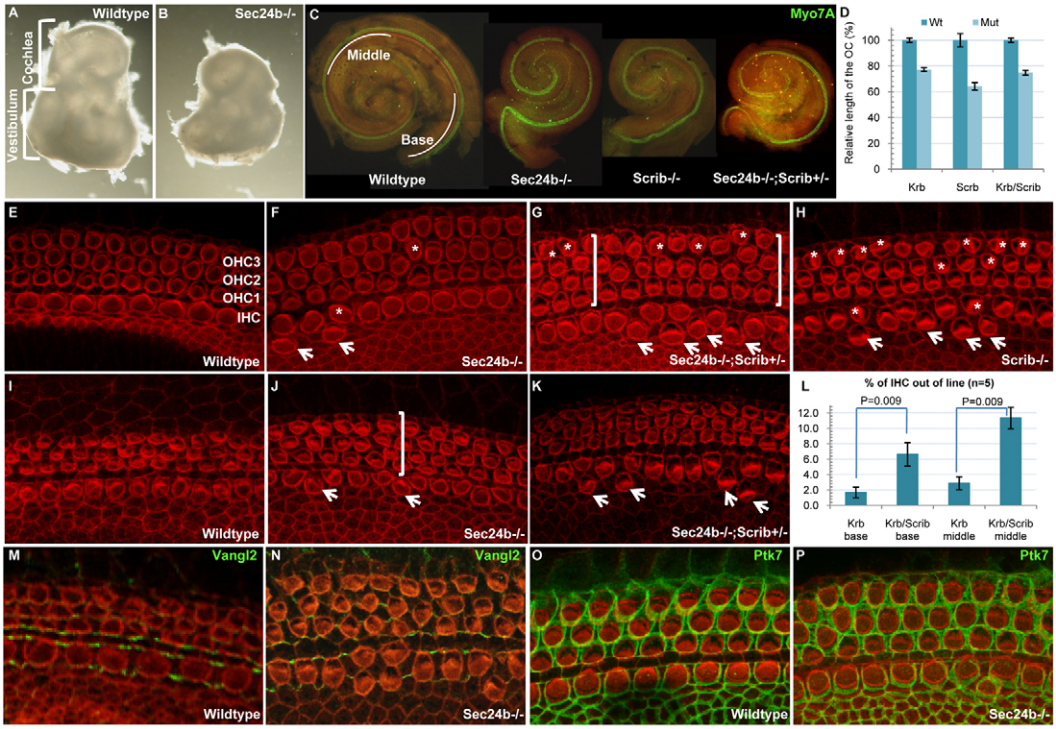

Fig. 3. Abnormal inner ear phenotype in *Sec24b*^{krabbel} mutants. (**A-D**) *Sec24b*^{krabbel} mutant embryos have a shorter cochlear duct as shown in external view (A,B; note relatively normal vestibular system). This was quantified by immunostaining of the hair cell marker Myo7A in the cochleae of the genotypes indicated (C). The length of this expression domain provides an objective measure for length reduction of the organ of Corti and indirectly for that of the cochlear duct. White lines in C indicate definition of the basal and middle regions used in the counting of abnormal cells. (D) Histogram revealing significantly shorter Myo7A domains in *Sec24b*$^{-/-}$ (Krb), *Scrib*$^{-/-}$ (*Scrib*) and *Sec24b*$^{-/-}$; *Scrib*$^{+/-}$ (Krb/Scrib) mutant cochleae compared with wild-type (Wt) cochlea. Mut, mutant. (**E-K**) Phalloidin stainings of F-actin in the stereocilia. Confocal *z*-stack images of the basal (E-H) and middle (I-K) part of the organ of Corti of wild-type (E,I), *Sec24b*$^{-/-}$ (F,J), *Sec24b*$^{-/-}$; *Scrib*$^{+/-}$ (G,K) and *Scrib*$^{-/-}$ (H) hair cells in the organ of Corti. Arrows indicate inner hair cells (IHC) that are out of line and asterisks in F-H indicate misoriented hair cells. Square brackets (G,J) indicate supernumerary rows of outer hair cells (OHC). (**L**) Histogram representing the quantification of results illustrated in E-K, demonstrating that the phenotype in *Sec24b*$^{-/-}$; *Scrib*$^{+/-}$ embryos is more severe than in *Sec24b*$^{-/-}$ embryos in the middle as well as the basal part of the cochlea, thus demonstrating genetic interaction between *Sec24b* and *Scrib*. *P*-values refer to statistical calculations comparing the results of countings for single mutants versus compound mutants as indicated by brackets. Abbreviations as in D. (**M-P**) Normal subcellular localization of Vangl2 (M,N) and Ptk7 (O,P) in supporting cells and hair cells. In D and L, error bars indicate standard error of the mean.

bundle orientation, as at this stage PCP is normally manifest from an asymmetrical localization of the kinocilium establishing a precisely oriented chevron arrangement of stereociliary bundles towards the abneural side of the sensory epithelium (Rida and Chen, 2009).

Phalloidin staining of the dissected organ of Corti at E17.5 at basal (Fig. 3E-H) and middle (Fig. 3I-K) regions (as defined by white lines in Fig. 3C) of the cochlear duct of wild types confirmed this highly organized pattern (Fig. 3E,I), but in the cochleae of mutants, a significant degree of disorganization was observed. Locally, a fourth row (Fig. 3G,J; square brackets) of outer hair cells appeared, or only two rows were seen (data not shown). In the single row of inner hair cells, cells were frequently positioned out of line (Fig. 3F,J; arrows). In addition, in the three rows of outer hair cells, stereociliary bundle orientation appeared to be rather frequently misaligned (Fig. 3F; asterisks). The severity of these aspects of the *Sec24b*^{krabbel} phenotype were mild compared with those reported for the PCP mutants mentioned above (Wang et al., 2005; Etheridge et al., 2008) and with *Scrib*^{51206} (Fig. 3H). In conclusion, a rather severe external abnormality of the cochlea is accompanied by a relatively mild phenotype in the organ of Corti.

Genetic interaction between *Sec24b*^{krabbel} and *Scrib*^{51206}

Evidence for involvement of two genes in a common pathway can be obtained by asking whether their phenotypes increase synergistically in double mutants. We crossed *Sec24b* mutants with the *Scrib*^{51206} mice, as well as with *Vangl2*^{looptail} mice (Kibar et al., 2001), but no neural tube defects were seen in either type of double-heterozygous embryos. Also, in other aspects of the phenotype, *Sec24b*/*Scrib* double-heterozygotes were indistinguishable from wild-type embryos. However, Merte and colleagues (Merte et al. 2010), using their *Sec24b* mutant line, reported significant incidence of open neural tube in *Sec24b*/*Vangl2* double-heterozygous embryos, confirming a link with PCP signaling. As both *Sec24b* mutants are almost certainly nulls, differences in the genetic backgrounds of the mice involved are the most probable explanation for this unexpected disparity.

We then analyzed embryos that were homozygous for *Sec24b*^{krabbel} and heterozygous for *Scrib*^{51206}. The neural tube defect of the *Sec24b* mutant, already extreme in single mutants, did not further deteriorate. Analyses of the cochleae from these compound mutants, however, showed significant differences, although these

were not evident from measurements of the Myo7A domains (Fig. 3C,D). We compared phenotypes in basal and middle areas of cochleae from these *Sec24b*$^{krabbel-/-}$; *Scrib*$^{51260+/-}$ embryos (Fig. 3G,K) with those of wild-type (Fig. 3E,I) and *Scrib*$^{51206+/-}$ (data not shown) embryos, as well as with *Sec24b*$^{krabbel-/-}$ embryos (Fig. 3F,J). Although Phalloidin stainings of *Scrib*$^{51206+/-}$ and wild-type hair cell patterns were indistinguishable, Phalloidin staining patterns seen in *Scrib*$^{51206+/-}$; *Sec24b*$^{krabbel-/-}$ organs of Corti revealed stronger disruption of hair cell alignment than in those of *Sec24b*$^{krabbel-/-}$, as was particularly evident in the inner ear cell row. Quantification of this effect was performed by counting the occurrence of abnormal inner hair cells in subsets of 70-130 cells from basal and middle regions of five cochlear ducts of both genotypes. The results, summarized in Fig. 3L, indicate higher percentages of abnormally positioned cells in the compound mutants compared with homozygous *Sec24b*^{krabbel} mutants. We quantified the effect by counting, for each individual row of cells separately, the percentage of cells that were misoriented by 30° either left or right. This revealed, as shown in Fig. S2 in the supplementary material, significantly higher percentages of misoriented cells in the single row of inner hair cells. In the three outer hair cell rows, differences were not statistically significant, although only by a narrow margin for row 3. To avoid ambiguity in cell row identification, we did not include cells of regions where an abnormal number of inner hair cells occurred; this might have had some impact on the numbers.

Therefore, removing one *Scrib* allele from a wild-type background is not enough to bring on an affected phenotype, but removing it from a *Sec24b*$^{krabbel-/-}$ background aggravates the phenotype. Involvement of *Scrib* in PCP signaling, suggested by its PCP-like phenotype, has been established by demonstrating genetic and physical interaction between *Scrib* and the PCP-core gene *Vangl2* (Montcouquiol et al., 2003; Montcouquiol et al., 2006). Their *Drosophila* orthologs *Scrib* and *Stbm*/*Vang* were recently shown to interact genetically and physically as well (Courbard et al., 2009). Genetic interaction with *Scrib* therefore implicates *Sec24b* in the PCP signaling pathway.

How does *Sec24b* link protein trafficking to planar polarity?

Having concluded that inactivation of *Sec24b* leads to disruption of the PCP pathway we asked the question of how deficiency of a COPII coat protein could lead to a defect in cell polarity. It would seem probable that this must somehow reflect a disruption of regulated protein trafficking. As Sec24 proteins are known to be involved in cargo selection (Mancias and Goldberg, 2008), an obvious hypothesis would be that transport of PCP-related membrane proteins depends relatively strongly on the Sec24b subunit. To test this possibility directly, we investigated the subcellular location of the PCP proteins Vangl2 and Ptk7 in two tissues that are affected by the *Sec24b* mutation, the presumptive neural tube around the 3-8 somite stage, at the onset of neurulation, and the organ of Corti at E17.5.

Wholemount immunolocalization demonstrated that Vangl2 is expressed throughout the presumptive neural tube of wild-type and heterozygous *Sec24b*^{krabbel} E8.25 embryos and localizes to the plasma membrane in wild types (Fig. 4A-C; see also Fig. S5A-I; Fig. S3A-C in the supplementary material).

By contrast, in neural folds of E8.25 homozygous mutant *Sec24b*^{krabbel} embryos, we detected abnormal Vangl2 expression or localization (Fig. 4D-F; see also Fig. S5J-R; Fig. S3D-F in the supplementary material). As these neural cells have large nuclei surrounded by a relatively thin shell of cytoplasm, it is not trivial to distinguish location to the plasma membrane from cytoplasmic location. We used an antibody against E-cadherin to demarcate the plasma membrane. At higher magnifications, a distinctly different

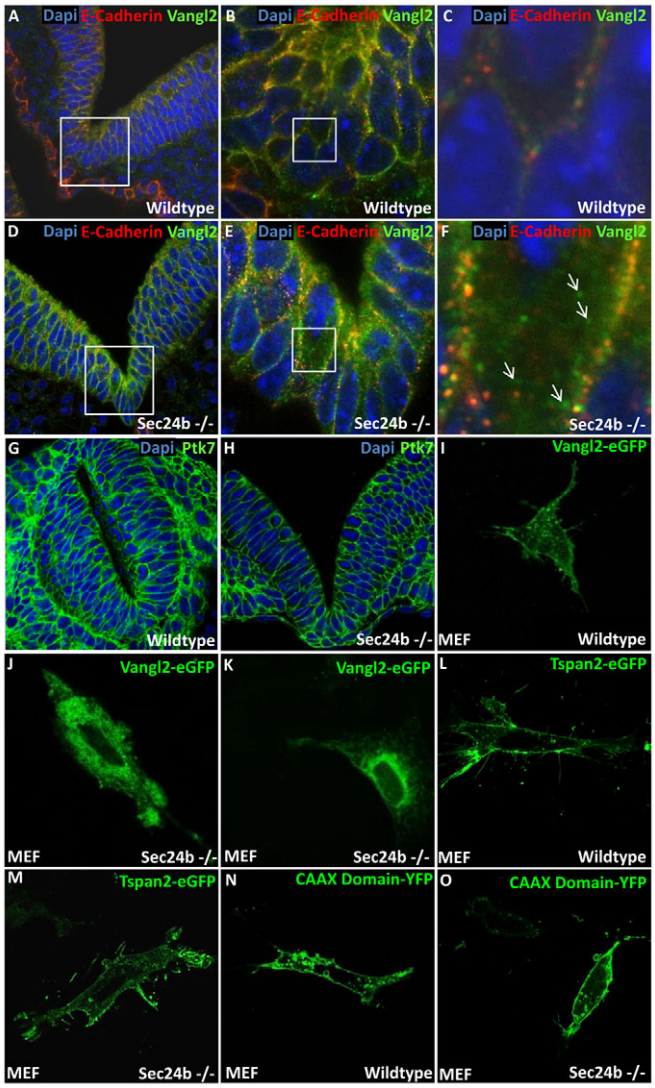

Fig. 4 The *Sec24b*^{krabbel} mutation affects trafficking of Vangl2, but not of membrane proteins. (**A-F**) Immunolocalization of Vangl2 (green) and E-cadherin (red) in confocal sections made of transverse vibratome sections. A-C and D-F represent increasing magnifications of the same section, as indicated by white squares. The space between nuclei (blue, DAPI) is so narrow that it requires the highest magnification (C,F) to demonstrate that E-cadherin and Vangl2 co-localize to the membrane in wild-type (A-C), but not *Sec24b*$^{-/-}$ (D-F), neural tube cells. Arrows in F indicate examples of Vangl2 staining not localized to the plasma membrane. For the individual fluorescence channels, see Fig. S5 in the supplementary material. (**G**,**H**) The PCP-related protein Ptk7 localizes to the plasma membrane both in wild-type and *Sec24b*$^{-/-}$ neural tube cells. (**I-O**) Defective ER exit of Vangl2 but not two different membrane proteins, demonstrated in *Sec24b*$^{-/-}$ primary fibroblasts. Transfection with a DNA construct encoding a Vangl2-eGFP fusion protein of MEFs prepared from wild-type (I) or *Sec24b*$^{-/-}$ (J,K) foetuses. Accumulation of fluorescent signal at the plasma membrane was seen in 75% of individual wild-type cells and never in mutant cells. Normal location was observed of a Tspan2-eGFP fusion protein (L,M) and a CAAX-domain-YFP fusion (N,O) in wild-type (L,N) and mutant (M,O) MEFs.

location is seen of E-cadherin (red signal in Fig. 4A-F) and Vangl2 (green). Arrows in Fig. 4F indicate examples of Vangl2 staining not located at the plasma membrane, which is not seen in wild-type embryos (Fig. 4C). In other experiments, the level of detected Vangl2 appeared to be lower in mutant neural folds (see Fig. S3 in the supplementary material). Staining of the PCP-related protein Ptk7 was identical in mutant and wild-type neural folds (Fig. 4G,H).

Hypothetically, the affected phenotype of the mutant could have consequences leading indirectly to abnormal behaviour of the Vangl2 protein. To confirm that abnormal Vangl2 location is not caused by such a 'downstream' effect, we show normal Ptk7 (see Fig. S4E-H,K,L in the supplementary material) and Vangl2 (see Fig. S4A-D,I,J in the supplementary material) protein location in cells in the neural folds of E8.5 *Scrib*$^{-/-}$ embryos and E17.5 *Scrib*$^{-/-}$ cochleae.

In the organ of Corti, where, as shown above, the phenotype is relatively mild, we observed normal Ptk7 staining patterns in wild-type embryos and *Sec24b* mutants (Fig. 3O,P). The Vangl2 protein was detected mostly in supporting cells and no convincing differences between wild types and mutants were seen, neither in subcellular location nor in overall levels (Fig. 3M,N). Accumulated Vangl2 is at this stage relatively easy to detect in supporting cells, whereas it is more difficult to perceive hair cells where it is more diffusely located. More appropriate stages to analyze this aspect of the phenotype are unfortunately beyond the lethal stage (around E17.5) of this mutant. Patterning of the organ of Corti at E17.5 is immature and membrane-bound Vangl2 is difficult to detect.

Transport of Sec24b is impeded in mutant primary fibroblasts

To corroborate these results with a methodologically independent approach, we transfected primary embryonic fibroblasts (MEFs) prepared from wild-type and *Sec24b*^{krabbel} mutant embryos with a Vangl2-eGFP fusion construct (Montcouquiol et al., 2006). An advantage of these cells is the larger volume of the cytoplasm, making the distinction between cell membrane and cytoplasm easier to detect. In approximately 75% of Vangl2-eGFP-transfected wild-type cells (as judged from the presence of any detectable fluorescence at all), the fluorescent signal clearly demarcated the plasma membrane, often in addition to its diffuse presence throughout the cytoplasm (Fig. 4I).

By contrast, in mutant MEFs this signal at the plasma membrane was never seen in three experiments performed in duplicate (Fig. 4J,K). The cytoplasmic fluorescence in these mutant cells was in some cases more strongly concentrated in areas surrounding the nucleus. Transfection with two additional constructs encoding fusion proteins known to localize to the plasma membrane, Tspan2-eGFP and CAAX-YFP resulted, as expected, in clear fluorescent signal at the plasma membrane (Fig. 4L-O) of MEFs of both genotypes. These data therefore confirm a defect in transport of the Vangl2 protein to the cell membrane.

Conclusions

Our observations show that loss-of-function of *Sec24b* leads to developmental defects affecting the spinal cord, the heart and the inner ear, resulting in a phenotype characteristically seen in mutants deficient for components of the PCP signaling pathway. We demonstrate that in mutant neural tube cells, as well as in mutant MEFs, the PCP core protein Vangl2 fails to locate to the cell membrane, presumably because of defective export from the ER. Absence of Vangl2 from the cell membrane is responsible for, or at least contributes to, the development of craniorachischisis. This observation indicates a surprising level of specificity in the mechanism of selective cargo exit from the ER. Even if, as we cannot exclude, transport of additional PCP proteins like Vangl1 is also compromised, the absence of other obvious defects in *Sec24b* mutants makes this a remarkably restricted phenotype. Interestingly, strong evidence for physical interaction between *Vangl2* and *Scrib* (Montcouquiol et al., 2003; Montcouquiol et al., 2006) and their *Drosophila* orthologs (Courbard et al., 2009) indicates that aberrant Vangl2 localization might also have an effect on the function of Scrib, even though this non-membrane protein is not expected itself to depend on ER-to-Golgi trafficking.

Clearly, functional Vangl2 deficiency is not complete, as is evident from the weaker phenotype in the organ of Corti and heart of *Sec24b* mutants compared with *Vangl2* mutants, as well as from our protein localization studies. The milder heart and ear phenotypes also suggest that in those tissues other factors, possibly other Sec24 isoforms, contribute to the specificity of cargo selection or that other PCP components like Vangl1 reach higher levels and are therefore better capable to compensate the phenotype.

Acknowledgements

This work was supported by a grant from the Netherlands government (BSIK program 03038, Stem Cells in Development and Disease). C.W. was the recipient of a Development Journal Traveling Fellowship. We thank Jeroen Korving for histology, Léon van Gurp for technical assistance, Martijn Koppens for doing some of the in situ experiments, Dr Xiaowei Lu for the gift of Ptk7 antibody, Jeroen Bussmann for a gift of CAAX-YFP and Jacqueline Deschamps for comments on the manuscript. We are also indebted to Stieneke van de Brink, Harry Beghtel and Marc van de Wetering for technical advice. Finally, we thank the Hubrecht Imaging Center for supporting the imaging.

Competing interests statement

The authors declare no competing financial interests.

Supplementary material

Supplementary material for this article is available at
http://dev.biologists.org/lookup/suppl/doi:10.1242/dev.041434/-/DC1

References

Albertson, R., Chabu, C., Sheehan, A. and Doe, C. Q. (2004). Scribble protein domain mapping reveals a multistep localization mechanism and domains necessary for establishing cortical polarity. *J. Cell Sci.* **117**, 6061-6070.

Copp, A. J., Greene, N. D. and Murdoch, J. N. (2003). The genetic basis of mammalian neurulation. *Nat. Rev. Genet.* **4**, 784-793.

Curtin, J. A., Quint, E., Tsipouri, V., Arkell, R. M., Cattanach, B., Copp, A. J., Henderson, D. J., Spurr, N., Stanier, P., Fisher, E. M. et al. (2003). Mutation of Celsr1 disrupts planar polarity of inner ear hair cells and causes severe neural tube defects in the mouse. *Curr. Biol.* **13**, 1129-1133.

Courbard, J.-R., Djiane, A., Wu, J. and Mlodzik, M. (2009). The apical/basal-polarity determinant Scribble cooperates with the PCP core factor Stbm/Vang and functions as one of its effectors. *Dev. Biol.* **333**, 67-77.

Davis, E. E. and Katsanis, N. (2007). Cell polarization defects in early heart development. *Circ. Res.* **101**, 122-124.

Devenport, D. and Fuchs, E. (2008). Planar polarization in embryonic epidermis orchestrates global asymmetric morphogenesis of hair follicles. *Nat. Cell Biol.* **10**, 1257-1268.

Etheridge, S. L., Ray, S., Li, S., Hamblet, N. S., Lijam, N., Tsang, M., Greer, J., Kardos, N., Wang, J., Sussman, D. J. et al. (2008). Murine dishevelled 3 functions in redundant pathways with dishevelled 1 and 2 in normal cardiac outflow tract, cochlea, and neural tube development. *PLoS. Genet.* **4,** e1000259.

Fromme, J. C., Orci, L. and Schekman, R. (2008). Coordination of COPII vesicle trafficking by Sec23. *Trends Cell Biol.* **18**, 330-336.

Henderson, D. J., Phillips, H. M. and Chaudhry, B. (2006). Vang-like 2 and noncanonical Wnt signaling in outflow tract development. *Trends Cardiovasc. Med.* **16**, 38-45.

Humbert, P., Russell, S. and Richardson, H. (2003). Dlg, Scribble and Lgl in cell polarity, cell proliferation and cancer. *BioEssays* **25**, 542-553.

Kasarskis, A., Manova, K. and Anderson, K. V. (1998). A phenotype-based screen for embryonic lethal mutations in the mouse. *Proc. Natl. Acad. Sci. USA* **95**, 7485-7490.

Kibar, Z., Vogan, K. J., Groulx, N., Justice, M. J., Underhill, D. A. and Gros, P. (2001). Ltap, a mammalian homolog of *Drosophila* Strabismus/Van Gogh, is altered in the mouse neural tube mutant Loop-tail. *Nat. Genet.* **28**, 251-255.
Kuehn, M. J. and Schekman, R. (1997). COPII and secretory cargo capture into transport vesicles. *Curr. Opin. Cell Biol.* **9**, 477-483.
Kuijper, S., Beverdam, A., Kroon, C., Brouwer, A., Candille, S., Barsh, G. and Meijlink, F. 2005. Genetics of shoulder girdle formation: roles of Tbx15 and aristaless-like genes. *Development* **132**, 1601-1610.
Lawrence, P. A., Struhl, G. and Casal, J. (2007). Planar cell polarity: one or two pathways? *Nat. Rev. Genet.* **8**, 555-563.
Lu, X., Borchers, A. G., Jolicoeur, C., Rayburn, H., Baker, J. C. and Tessier-Lavigne, M. (2004). PTK7/CCK-4 is a novel regulator of planar cell polarity in vertebrates. *Nature* **430**, 93-98.
Merte, J., Jensen, D., Wright, K., Sarsfield, S., Wang, Y., Schekman, R. and Ginty, D. D. (2010). Sec24b selectively sorts Vangl2 to regulate planar cell polarity during neural tube closure. *Nat. Cell Biol.* **12**, 41-46.
Mancias, J. D. and Goldberg, J. (2008). Structural basis of cargo membrane protein discrimination by the human COPII coat machinery. *EMBO J.* **27**, 2918-2928.
Montcouquiol, M., Rachel, R. A., Lanford, P. J., Copeland, N. G., Jenkins, N. A. and Kelley, M. W. (2003). Identification of Vangl2 and Scrb1 as planar polarity genes in mammals. *Nature* **423**, 173-177.
Montcouquiol, M., Sans, N., Huss, D., Kach, J., Dickman, J. D., Forge, A., Rachel, R. A., Copeland, N. G., Jenkins, N. A., Bogani, D. et al. (2006). Asymmetric localization of Vangl2 and Fz3 indicate novel mechanisms for planar cell polarity in mammals. *J. Neurosci.* **26**, 5265-5275.
Montcouquiol, M., Jones, J. M. and Sans, N. (2008). Detection of planar polarity proteins in mammalian cochlea. *Methods Mol. Biol.* **468**, 207-219.
Murdoch, J. N., Rachel, R. A., Shah, S., Beermann, F., Stanier, P., Mason, C. A. and Copp, A. J. (2001). Circletail, a new mouse mutant with severe neural tube defects: chromosomal localization and interaction with the loop-tail mutation. *Genomics* **78**, 55-63.
Murdoch, J. N., Henderson, D. J., Doudney, K., Gaston-Massuet, C., Phillips, H. M., Paternotte, C., Arkell, R., Stanier, P. and Copp, A. J. (2003). Disruption of scribble (Scrb1) causes severe neural tube defects in the circletail mouse. *Hum. Mol. Genet.* **12**, 87-98.
Rachel, R. A., Wellington, S. J., Warburton, D., Mason, C. A. and Beermann, F. (2002). A new allele of Gli3 and a new mutation, circletail (Crc), resulting from a single transgenic experiment. *Genesis* **33**, 55-61.
Rida, P. C. and Chen, P. (2009). Line up and listen: Planar cell polarity regulation in the mammalian inner ear. *Semin. Cell. Dev. Biol.* **20**, 978-985.
Saburi, S., Hester, I., Fischer, E., Pontoglio, M., Eremina, V., Gessler, M., Quaggin, S. E., Harrison, R., Mount, R. and McNeill, H. (2008). Loss of Fat4 disrupts PCP signaling and oriented cell division and leads to cystic kidney disease. *Nat. Genet.* **40**, 1010-1015.
Salama, N. R. and Schekman, R. W. (1995). The role of coat proteins in the biosynthesis of secretory proteins. *Curr. Opin. Cell Biol.* **7**, 536-543.
Sato, A. and Nakano, A. (2007). Mechanisms of COPII vesicle formation and protein sorting. *FEBS Lett.* **581**, 2076-2082.
Stalder, L. and Muhlemann, O. (2008). The meaning of nonsense. *Trends Cell Biol.* **18**, 315-321.
Torban, E., Patenaude, A. M., Leclerc, S., Rakowiecki, S., Gauthier, S., Andelfinger, G., Epstein, D. J. and Gros, P. (2008). Genetic interaction between members of the Vangl family causes neural tube defects in mice. *Proc. Natl. Acad. Sci. USA* **105**, 3449-3454.
van den Hoff, M. J. and Moorman, A. F. (2005). Wnt, a driver of myocardialization? *Circ. Res.* **96**, 274-276.
van Nes, J., De Graaff, W., Lebrin, F., Gerhard, M., Beck, F. and Deschamps, J. (2006). The Cdx4 mutation affects axial development and reveals an essential role of Cdx genes in the ontogenesis of the placental labyrinth in mice. *Development* **133**, 419-428.
Wang, J., Mark, S., Zhang, X., Qian, D., Yoo, S. J., Radde-Gallwitz, K., Zhang, Y., Lin, X., Collazo, A., Wynshaw-Boris, A. et al. (2005). Regulation of polarized extension and planar cell polarity in the cochlea by the vertebrate PCP pathway. *Nat. Genet.* **37**, 980-985.
Wang, Y. and Nathans, J. (2007). Tissue/planar cell polarity in vertebrates: new insights and new questions. *Development* **134**, 647-658.
Wendeler, M. W., Paccaud, J. P. and Hauri, H. P. (2007). Role of Sec24 isoforms in selective export of membrane proteins from the endoplasmic reticulum. *EMBO Rep.* **8**, 258-264.
Wu, J. and Mlodzik, M. (2009). A quest for the mechanism regulating global planar cell polarity of tissues. *Trends Cell Biol.* **19**, 295-305.
Zarbalis, K., May, S. R., Shen, Y., Ekker, M., Rubenstein, J. L. and Peterson, A. S. (2004). A focused and efficient genetic screening strategy in the mouse: identification of mutations that disrupt cortical development. *PLoS Biol.* **2**, E219.
Zhan, L., Rosenberg, A., Bergami, K. C., Yu, M., Xuan, Z., Jaffe, A. B., Allred, C. and Muthuswamy, S. K. (2008). Deregulation of scribble promotes mammary tumorigenesis and reveals a role for cell polarity in carcinoma. *Cell* **135**, 865-878.

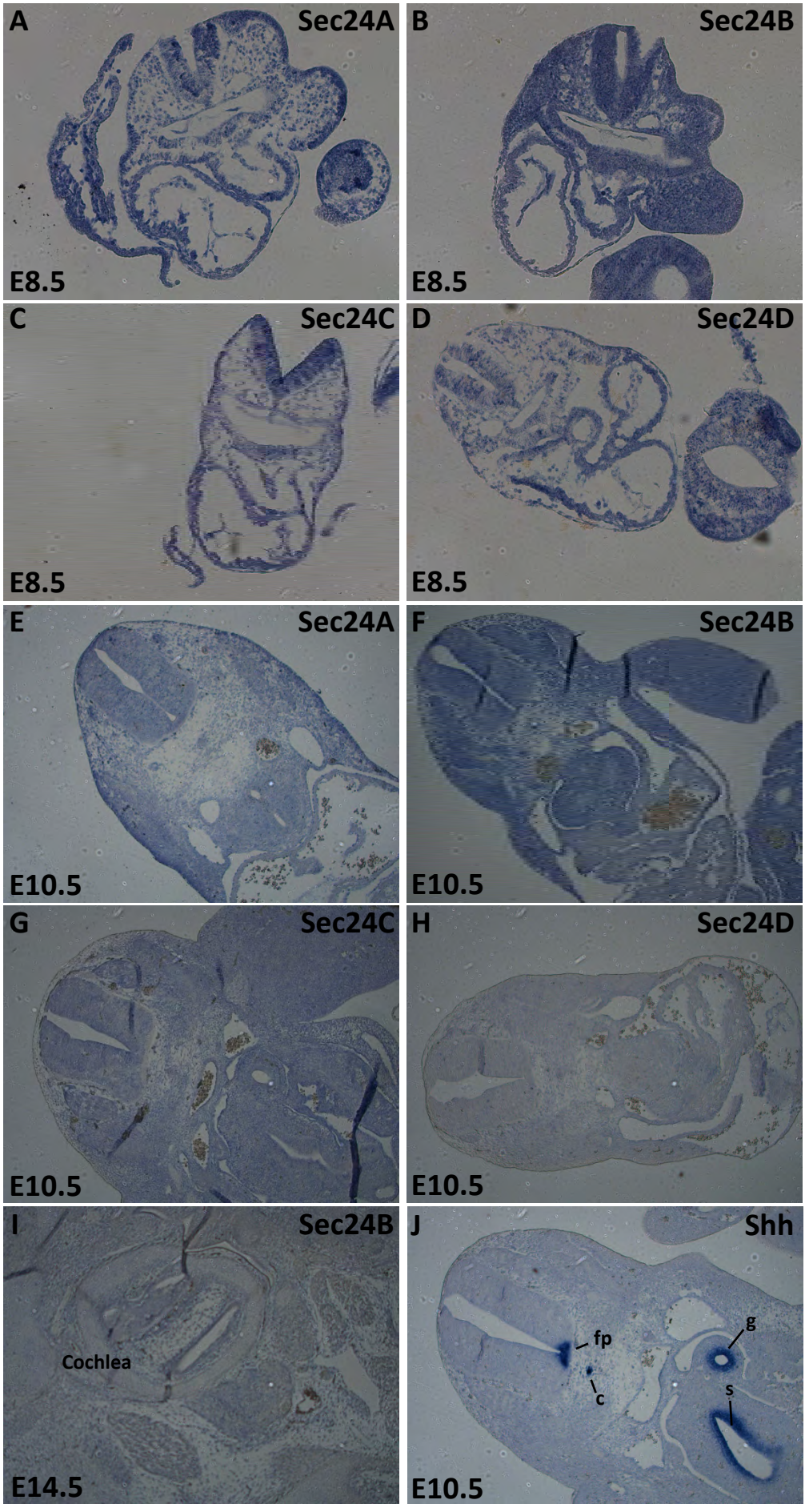
A
Sec24A
E8.5
B
Sec24B
E8.5
C
Sec24C
E8.5
D
Sec24D
E8.5
E
Sec24A
E10.5
F
Sec24B
E10.5
G
Sec24C
E10.5
H
Sec24D
E10.5
I
Sec24B
Cochlea
E14.5
J
Shh
fp
g
c
s
E10.5

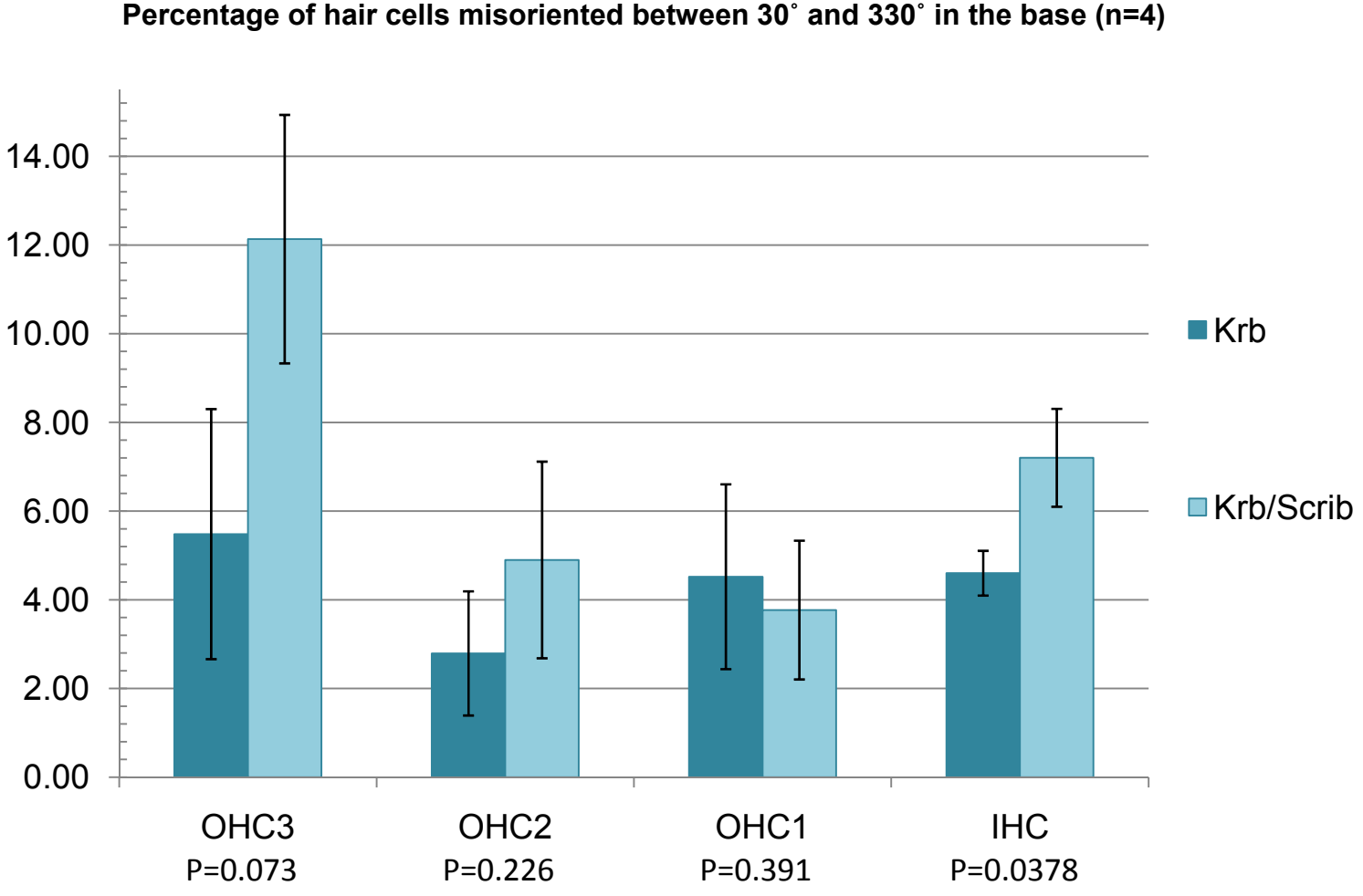
Percentage of hair cells misoriented between 30˚ and 330˚ in the base (n=4)
14.00
12.00
10.00
8.00
6.00
4.00
2.00
0.00
Krb
Krb/Scrib
OHC3
P=0.073
OHC2
P=0.226
OHC1
P=0.391
IHC
P=0.0378

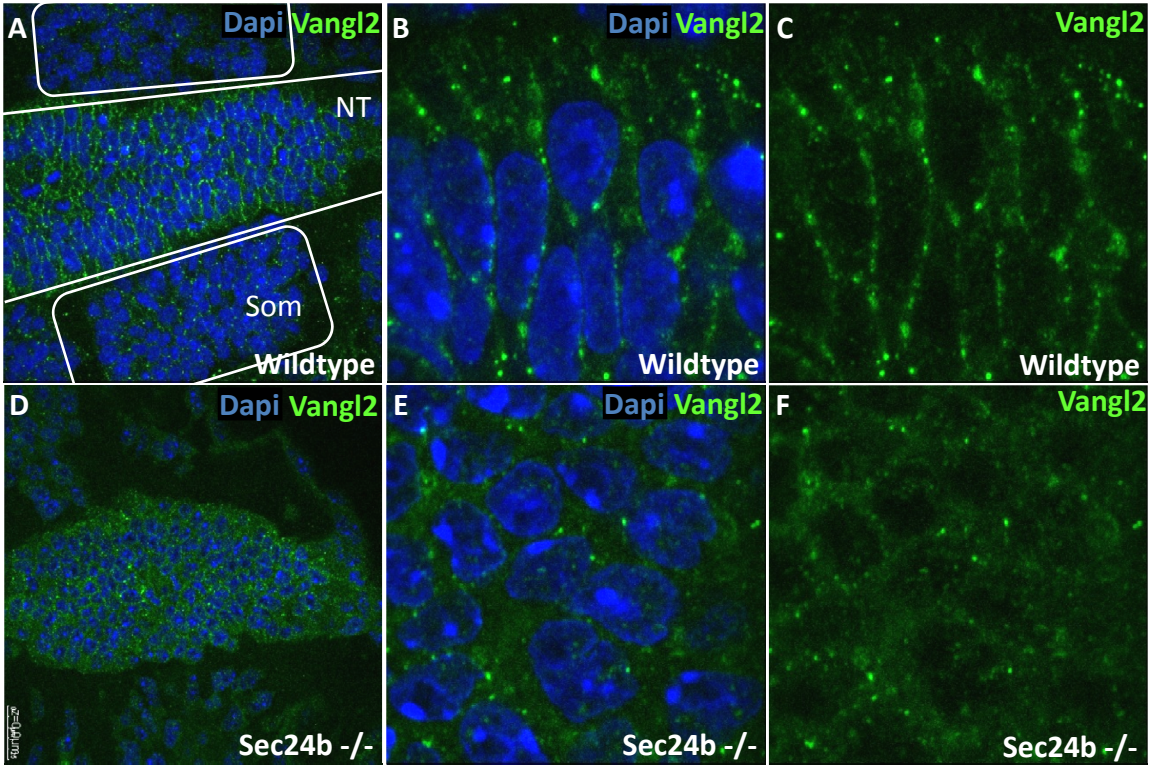
A
Dapi Vangl2
NT
Som
Wildtype
B
Dapi Vangl2
Wildtype
C
Vangl2
Wildtype
D
Dapi Vangl2
Sec24b -/-
E
Dapi Vangl2
Sec24b -/-
F
Vangl2
Sec24b -/-

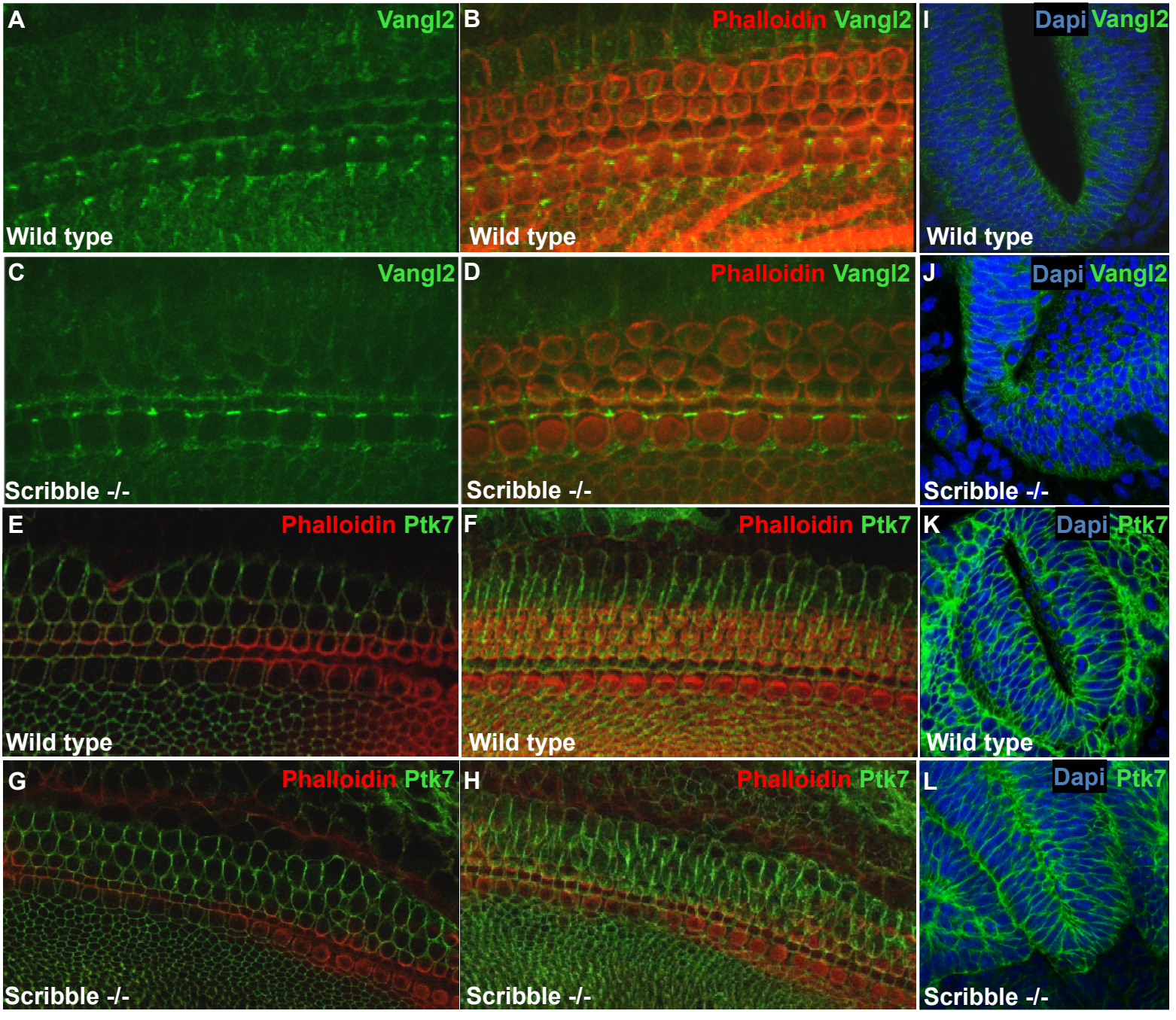
A
Vangl2
Wild type
B
Phalloidin Vangl2
Wild type
I
Dapi Vangl2
Wild type
C
Vangl2
Scribble -/-
D
Phalloidin Vangl2
Scribble -/-
J
Dapi Vangl2
Scribble -/-
E
Phalloidin Ptk7
Wild type
F
Phalloidin Ptk7
Wild type
K
Dapi Ptk7
Wild type
G
Phalloidin Ptk7
Scribble -/-
H
Phalloidin Ptk7
Scribble -/-
L
Dapi Ptk7
Scribble -/-

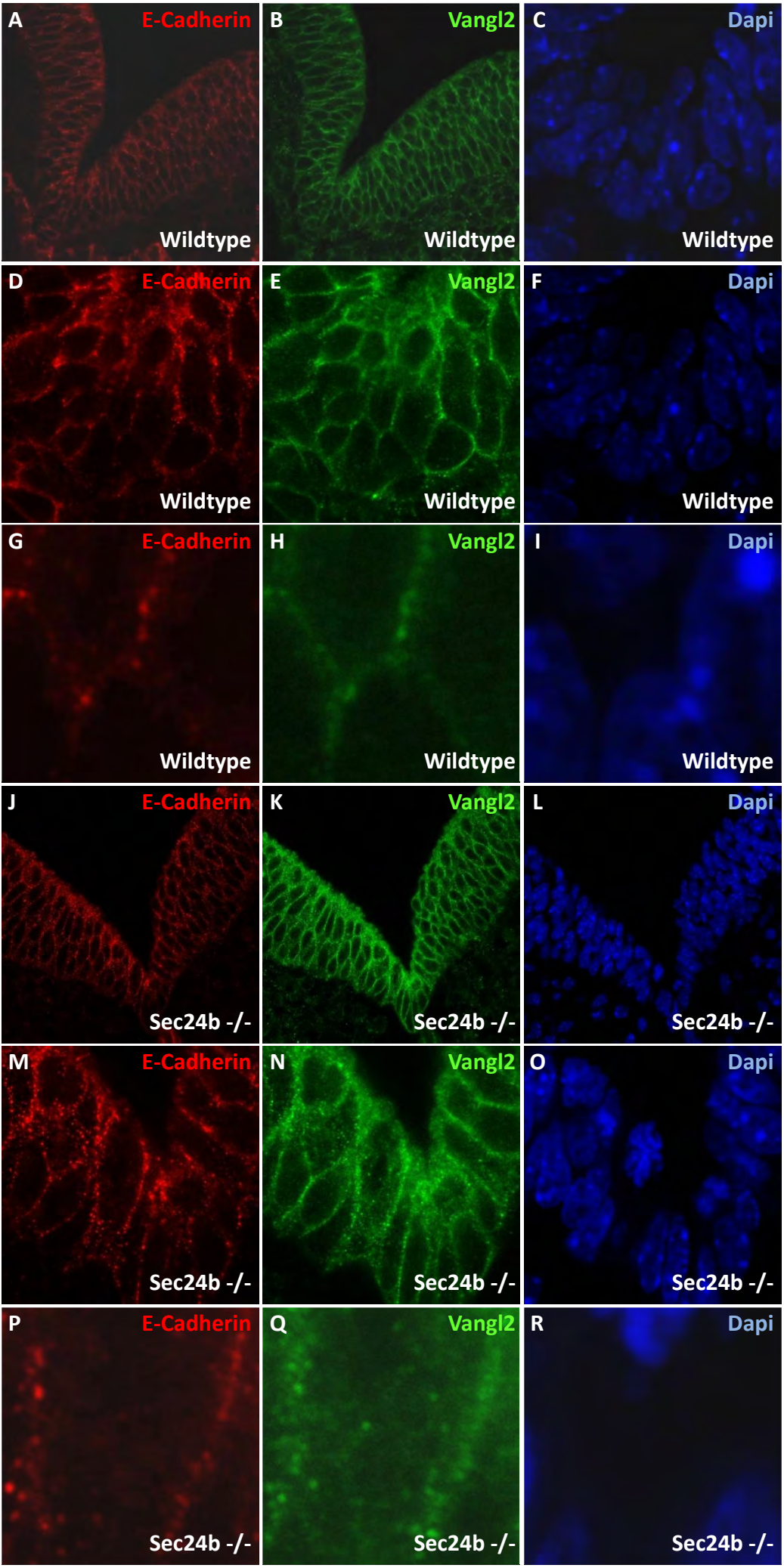
A
E-Cadherin
Wildtype
B
Vangl2
Wildtype
C
Dapi
Wildtype
D
E-Cadherin
Wildtype
E
Vangl2
Wildtype
F
Dapi
Wildtype
G
E-Cadherin
Wildtype
H
Vangl2
Wildtype
I
Dapi
Wildtype
J
E-Cadherin
Sec24b -/-
K
Vangl2
Sec24b -/-
L
Dapi
Sec24b -/-
M
E-Cadherin
Sec24b -/-
N
Vangl2
Sec24b -/-
O
Dapi
Sec24b -/-
P
E-Cadherin
Sec24b -/-
Q
Vangl2
Sec24b -/-
R
Dapi
Sec24b -/-